Pergamon

Journal of Structural Geology, Vol. 19, Nos 3–4, pp. 535 to 550, 1997

0191-8141/97 $17.00 + 0.00

PII: S0191-8141(96)00099-5

Three-dimensional geometry, strain rates and basement deformation mechanisms of thrust-bend folding

CHRISTOPHER A. J. WIBBERLEY*

Department of Earth Sciences, University of Leeds, Leeds LS2 9JT, U.K.

(*Received* 5 *February* 1996; *accepted in revised form* 10 *October* 1996)

Abstract—Models for thrust-bend folding of an isotropic medium are used to predict initial basement thrust sheet geometries and sub-surface thrust fault shapes from final basement thrust sheet structure. Predicted strains and strain rates from these models are compared with data on deformation fabrics in an example of a basement thrust-bend fold in order to characterise the deformation response to thrust-bend folding. The Glencoul thrust sheet in the Moine Thrust Zone of north-west Scotland is restored to an initial thrust sheet geometry. Spatial and orientation distribution data of syn-emplacement fractures and cataclastic fault zones from within the Glencoul thrust sheet are then compared with the strain and strain rate histories predicted by thrust-bend folding models. A different set of cataclastic fault seams is demonstrated to have been generated at each frontal thrust bend. Cataclastic failure is restricted to portions of the thrust sheet that have moved over frontal bends with smaller radii of curvature. From model thrust-bend geometries and an assumed slip rate of 1×10^{-10} m s^{-1}, estimated minimum (critical) strain rates required for fracture failure of the Lewisian basement are 10^{-11} to 10^{-14} s^{-1} for shear strain rates and 10^{-12} to 10^{-15} s^{-1} for extensional strain rates. © 1997 Elsevier Science Ltd. All rights reserved.

INTRODUCTION

This paper addresses the basic relationships between the geometry of the thrust surface and the operative deformation mechanisms within a basement thrust sheet. Numerous reviews of thrust geometries (Boyer and Elliott, 1982; Butler, 1982a; McClay, 1992) discuss how and why thrusts are typically not planar, but follow datum parallel flats (often weak lithological horizons such as shale or evaporite), before climbing up through more competent units in the stratigraphic section as ramps to link with a higher flat to result in a 'staircase geometry'. A thrust sheet deforms as it is emplaced over such bends in the thrust surface (Wiltschko, 1979; Berger and Johnson, 1980; Fischer and Coward, 1982; Sanderson, 1982; Suppe, 1983; Knipe, 1985; Mitra, 1992b). This produces thrust-bend folds, or folds between hanging wall ramps and hanging wall flats.

The purpose of this paper is to relate the distribution of deformation and deformation mechanisms within basement thrust sheets to the evolution of geometry, strain and strain rate in thrust-bend folds. In order to do this, other causes of syn-emplacement thrust sheet deformation need to be considered, so that their possible roles in contributing to the generation of structures may be invoked or eliminated. In addition to fault-bend folding (Rich, 1934; Suppe, 1983; Mitra, 1992b), these include: (1) fault propagation folding (Dahlstrom, 1969; Suppe and Medwedeff, 1984; Mitra, 1990; Mosar and Suppe, 1992), (2) detachment folding (Dahlstrom, 1970; Jamison, 1987), (3) buckle folding due to initial ramp resistance (Serra, 1977; Hedlund *et al.*, 1994), (4) fault-parallel shear (Elliott, 1976a; Coward and Kim, 1981; Wojtal, 1992; Mitra, 1994) and (5) layer-parallel shortening (McNaught and Mitra, 1996). These and many other authors have described diagnostic characteristics of the deformation fabrics and thrust sheet geometries which allow the causative deformation processes to be identified. Deformation fabrics from basement thrust sheets have been described and often attributed to one or more of the above causes, the most frequently documented one being basement faulting associated with fault propagation folding (Erslev and Rogers, 1993; Narr, 1993). Whilst fruitful work has stemmed from comparing basement deformation geometries and fabrics to those of the cover (Dominic and McConnell, 1994), few detailed accounts exist of deformation mechanisms operating in basement during the synchronous evolution of frontal and lateral thrust-bend folds. The current paper aims to rectify this by evaluating the deformation fabrics in terms of the incremental strains and strain rates associated with thrust-bend frontal and lateral folding.

Previous investigations of the deformation mechanisms operating within basement thrust sheets have revealed a wide range of brittle to ductile mechanisms (Mitra, 1979, 1984, 1992a; Choukroune and Gapais, 1983; Bertini *et al.*, 1985; Evans, 1988, 1993; Hatcher and Hooper, 1992). However, in the foreland thrust zones of orogenic belts, where relatively low temperatures and confining pressures have accompanied deformation (Ernst, 1973; Frey *et al.*, 1974, 1993; Knipe, 1990; Meyre and Puschnig, 1993), cataclasis generally dominates (Evans, 1988, 1990; Spang and Evans, 1988; Mitra, 1992; Wibberley, 1995). This paper investigates the operative deformation mechanisms during emplacement of a basement thrust sheet within the foreland thrust zone of the Moine thrust belt, NW Scotland.

Geometric/strain models for deformation of isotropic

*Present address: Laboratoire de Geophysique et Tectonique, UMR CNRS, UM11 5573, Université Montpellier 11, 34095, France.

thrust sheets due to movement over footwall ramps are discussed and used to predict restored basement thrust sheet shapes, i.e. pre-emplacement 'retrodeformed' thrust sheet templates. The models are also used to predict quantified strain and strain rate histories of different regions within the thrust sheet. Data are presented on the orientation and spatial distributions of syn-emplacement fabrics within the Glencoul thrust sheet, and these data are used to interpret the deformation mechanisms operating in basement during thrust-bend folding. This paper also addresses the deformation mechanisms and the 3-D kinematics associated with lateral and frontal thrust-bend folding.

GEOMETRIC AND KINEMATIC MODELS OF THRUST-BEND FOLDING

This section shows how models for thrust sheet deformation may be used to estimate parameters such as original ramp dip, ramp length, shear strains and extensional or shortening strains from field data. These parameters may be used to place a thrust sheet in a simple restored or 'retrodeformed' shape and restore localities in the thrust sheet into their pre-emplacement position.

Thrust surface geometry and strain paths

A thrust surface may cut up-section along strike (perpendicular to the transport direction) at a lateral ramp (Fig. 1a). Cross-sections of a thrust sheet drawn perpendicular to the transport direction (lateral cross-sections) will change shape in the region around the lateral ramp, during movement over the frontal ramp. This shape change is illustrated in Fig. 1(b) which shows how the locus of deformation within the hanging wall lateral ramp moves outwards with time. This is because the 'corner' bend between the lateral and frontal ramps is orientated such that up-dip of the thrust ramp surface it is closer to the lateral cut-off line (Fig. 1a). Three regions can be defined within a thrust sheet which have been emplaced over different sequences of thrust bends, and therefore have different strain histories (Fig. 1a). The hanging wall ramp (initially overlying region 1 (Fig. 1a)) has moved over only the upper ramp/flat bend. The hanging wall flat (initially overlying region 2) has moved over both the lower flat/ramp and the upper ramp/flat bends. The hanging wall lateral ramp (initially overlying region 3) moved firstly over the frontal ramp/lateral ramp 'corner' bend, then moved over the upper frontal ramp/flat bend.

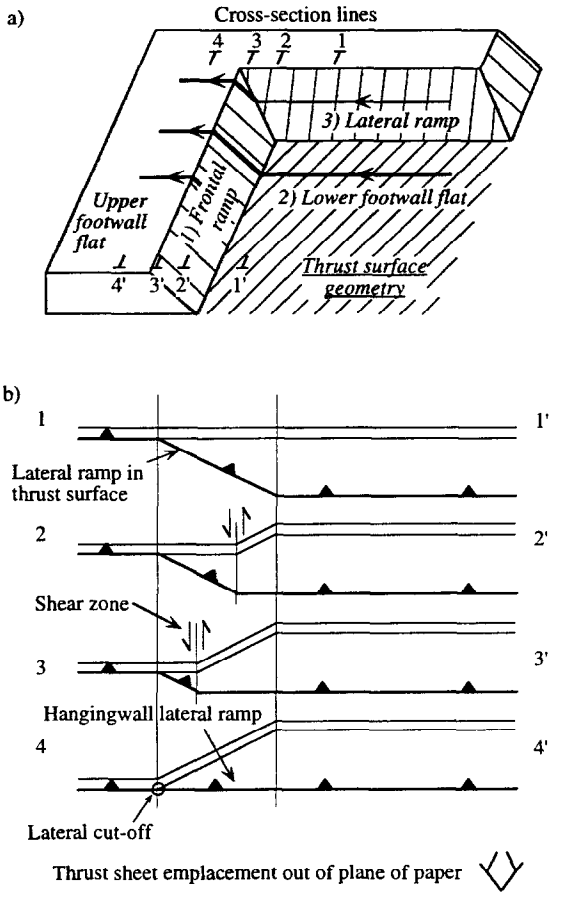

Fig. 1. (a) Cartoon of thrust surface geometry showing three different regions which have different histories of emplacement over thrust bends. (b) Geometric evolution of a thrust sheet lateral ramp during emplacement on an upper footwall flat, illustrated by hanging wall sequence diagrams (strike-parallel cross-sections).

Strains and strain rates involved in thrust-bend folding

Previous models for strain evolution and accommodation within hanging wall ramp anticlines generally rely on simple bedding anisotropies. These include the 'bending' or vertical shear model of Sanderson (1982), the bedding-parallel flexural shear model of Suppe (1983), and the model of inclined shear bisecting the ramp/flat angle with strains partitioned into bedding-parallel flexural shear and rotations (Fischer and Coward, 1982 and the 'flexural flow' model of Sanderson, 1982). The Suppe (1983) model is particularly reliant on bedding, constructed for the special case of no bed length extension, and is therefore considered inappropriate to models of basement deformation.

Most 2-D models for deformation above thrust bends envisage thrust sheet deformation by shear along a steeply inclined plane or zone (Fischer and Coward, 1982; Sanderson, 1982; Knipe, 1985), so that within the thrust sheet, relative movement is parallel to this plane only (Fig. 2a). Such deformation may be represented by a shear transformation, which is illustrated in terms of a relative velocity vector diagram (McCaig, 1988). This is identical to the technique used to analyse the kinematics of plate boundaries at triple junctions (Cox and Hart, 1986). A criticism of applying this technique to mesoscale fault zones is that wall rock adjacent to a fault may not behave rigidly in the same way as the macroscopic behaviour of the oceanic lithosphere (Apotria, 1989). Yet we may still

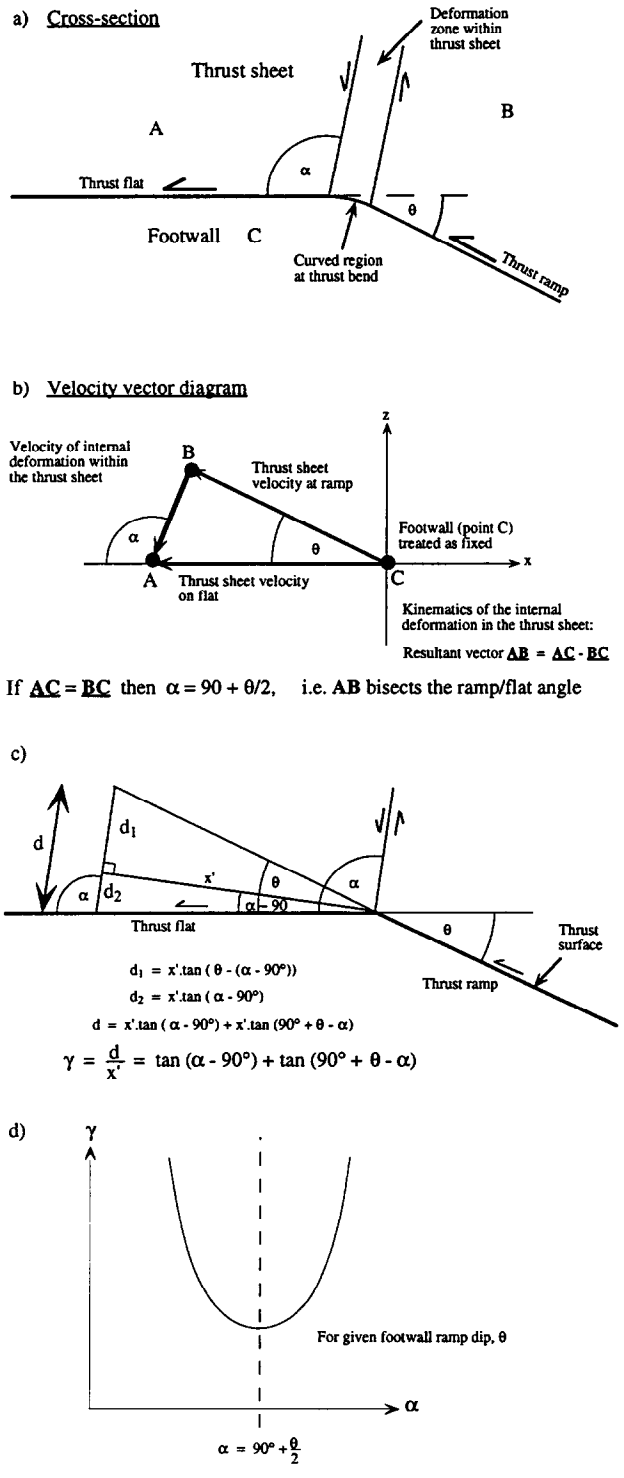

Fig. 2. (a) Thrust sheet deformation by steep shear zone acitivity above a thrust bend. (b) Use of relative velocity vector diagrams to assess the kinematics of internal thrust sheet deformation due to emplacement over thrust bends (after McCaig, 1988). (c) Derivation of shear strain magnitudes experienced by a thrust sheet due to motion over a ramp/flat thrust bend. (d) Graph of shear strain versus angle of shear zone, for a thrust sheet deforming above a thrust bend.

use relative displacement vectors (for any one time increment) to predict how a thrust sheet behaves non-rigidly (Fig. 2b). For an increment of time, Fig. 2(b) illustrates that for any given ramp dip (θ), the ratio of thrust sheet displacement at the ramp (BC) (relative to the footwall) to thrust sheet displacement at the flat (AC) (relative to the footwall) is interdependent with the magnitude of the displacement vector of internal deformation within the thrust sheet (AB) and the angle of the shear plane (α). The shear strain (γ) may be derived (Fig. 2c) in terms of ramp dip (θ) and shear plane angle (α):

$$\gamma = \tan(\alpha - 90°) + \tan(90° + \theta - \alpha). \quad (1)$$

Using equation (1), the relationship between shear strain (γ) and angle of the shear plane (α) is plotted in Fig. 2(d) for a given ramp dip (θ). Figure 2(d) shows that for an isotropic medium moving over a ramp/flat bend, the induced shear strain (γ) is at a minimum when $\alpha = 90° + \theta/2$, i.e. when the shear plane bisects the ramp/flat angle. In this case, $\gamma = 2 \cdot \tan\theta/2$ (Fischer and Coward, 1982; Sanderson, 1982). This is a simplification of equation (1), with $90° + \theta/2$ substituted for α. The mathematical transformations which represent these steep shear strains are equivalent to layer-parallel flexural shear strains and rotations by $\theta°$. This note shows how a velocity vector analysis is compatible with the layer-parallel shear models of Fischer and Coward (1982), Sanderson (1982) ('flexural flow' model) and Suppe (1983).

Knipe (1985) describes how bends in a thrust surface may not be sharp corners, but relatively smooth arcs, with a definable distance over which the thrust sheet is strained. Knipe also shows that the strain rate is a function of the curvature of the bend arc, and expresses this curvature in terms of the straining distance, (w): the higher the arc curvature (lower the straining distance), the faster the strain rate generated in the thrust sheet, and vice versa (for a given ramp dip, θ, and displacement rate, d). Hence an evaluation of thrust surface geometry is important in understanding the relative strain rate histories within the thrust sheet.

Prediction of initial thrust sheet geometries

Initial thrust sheet geometries may be obtained by 'retrodeforming' the thrust sheet (McNaught and Mitra, 1996). In this case only thrust-bend folding is considered in the process. The process restores the thrust sheet shape by steep simple shear in a manner described in Wibberley (1995), using relationships between initial ramp dip (θ) the final cut-off angle (θ') and angle of dip of the shear plane (α) (Suppe, 1983).

Because crystalline basement is generally either isotropic, or so heavily anisotropic that no preferred orientation of fabrics exist to give rise to any particular mechanical layering within the thrust sheet, basement thrust sheets are here treated as mechanically isotropic. Assuming that they will deform by the minimum shear strain possible, equation (1) shows that basement thrust sheets are most likely to deform by simple shear along a plane bisecting the ramp/flat transition, where $\alpha = 90° + \theta/2$. In this case, Wibberley (1995) showed that the relationship between final hanging wall ramp cut-off

angle (θ') and ramp dip (θ) can be expressed as:

$$\tan \theta' = \frac{1}{2 \cdot \tan \frac{\theta}{2} + \frac{1}{\tan \theta}} \quad (2)$$

Estimation of original vertical ramp height and the calculated original ramp dip may be used to create a restored thrust sheet geometry.

A similar exercise may be carried out for lateral cross-sections through a thrust sheet which has experienced shape changes due to emplacement of a hanging wall lateral ramp over a frontal ramp (Fig. 1b), forming a hanging wall lateral ramp monocline (Harris, 1970; Elliott and Johnson, 1980; Butler, 1982a). Investigations of the exact geometric evolution of thrust sheet lateral ramps are beyond the scope of this paper. For the purposes of restoring the Glencoul thrust sheet to its pre-emplacement geometry, a vertical shear model was used for the lateral cross-section because it maintained strain compatibility along strike. This model provides only approximate restored geometries, due to the possibility of more complex, non-plane strains (Apotria *et al.*, 1992; Apotria, 1995). Strains due to lateral folding are not modelled quantitatively here because of uncertainties in geometric evolution of the lateral fold.

In the following sections, the concepts detailed above are applied to the Glencoul thrust sheet of the Moine Thrust Zone.

THE GLENCOUL THRUST SHEET

Regional context

The Moine Thrust Zone (Elliott and Johnson, 1980; McClay and Coward, 1981) is a relatively narrow NNE–SSW trending linear thrust belt exposed for a length of 200 km on mainland NW Scotland (Fig. 3a). Within the evolution of the Moine Thrust Zone, the Glencoul thrust emplaced Lewisian basement west-northwest-wards along a basement lower flat, over a ramp within basement and Lower Cambrian Eriboll quartzite, and along an upper flat at the top of the quartzite (Figs 3c & 5a) with an estimated displacement of 25–35 km (Coward *et al.*, 1980; Elliott and Johnson, 1980). This process occurred at deformation conditions of approximately 250–300°C and 5–9 km depth of burial (Knipe, 1990).

The structure of the Glencoul thrust sheet

Lewisian basement in the middle of the Glencoul thrust sheet is overlain by Cambrian quartzites. The base of the quartzites was a planar unconformity prior to thrusting, and is important in defining thrust sheet structure (Elliott and Johnson, 1980). Figure 3(c) shows a map of the Glencoul thrust sheet, whose structure has been determined by structure contouring the thrust surface and the basement/cover contact (Elliott and Johnson, 1980; Wibberley, 1995) as shown in Fig. 4(a).

The Lewisian basement is exposed in the middle of the thrust sheet in a culmination. Cross-sections drawn through the middle of the basement culmination parallel to the emplacement direction illustrate that the thrust sheet has been folded through an angle of 20°, with a NNE–SSW trending horizontal fold axis (Fig. 5a) (Elliott and Johnson, 1980), in the style of a hanging wall ramp anticline (Rich, 1934). A final cut-off angle of 20° is much lower than that considered likely to have resulted from fault-propagation folding (Suppe and Medwedeff, 1984; Mitra, 1990; Mosar and Suppe, 1992), but is consistent with thrust-bend folding (Suppe, 1983; Mitra, 1992a).

Within most of the Glencoul thrust sheet, the basement/cover contact trends NNE–SSW, which is perpendicular to the emplacement direction of the thrust sheet. On the northern side of the basement outcrop, however, it trends parallel to the emplacement direction. This change in orientation has been interpreted (Peach *et al.*, 1907; Elliott and Johnson, 1980; Butler, 1984) as a lateral fold formed by emplacement of an initial hanging wall ramp onto a higher footwall flat. This lateral fold model predicts that the fold axis and the cut-off line of the bedding against the Glencoul thrust will both trend parallel to the bulk emplacement direction (Butler, 1982a,b). An original oblique ramp will result in an oblique cut-off line and an oblique fold-axis trend. The structure of the region is shown in Fig. 4, showing that the cut-off of the basement/cover contact by the Glencoul thrust surface (where determined from contour intersections) trends 060° and the fold axis of the folded basement/cover contact trends 080°. Given that the emplacement direction of the Glencoul thrust sheet is to the WNW (Elliott and Johnson, 1980), this suggests that the region is a hanging wall oblique ramp in the Glencoul thrust sheet, which changes east-wards into a hanging wall lateral ramp.

The Lewisian basement of the area comprises acidic to intermediate gneisses, with a centimetre scale gneissic banding cross-cut by pink 0.5–3 m wide pegmatite sheets. The presence of a lateral or oblique hanging wall fold in the basement can be tested by examining the geometry of the basement structures. Wibberley (1995) presents a detailed map of the Lewisian basement, based on 1:2000 scale mapping and foliation form tracing, which illustrates that the gneissic foliation is gradually folded over the same scale as the cover ($\sim$1 km on a NNE–SSW transect). There are also metre to tens of metres scale open folds of the gneissic foliation in each part of the area. Data on the gneissic foliation orientations are presented here in Fig. 4. The data presented in Fig. 4(b) suggest that the Lewisian basement was folded through 60° about an axis plunging 02° towards 112°. Similar effects of frontal hanging wall ramp anticline are not observed because the regional attitude of the Lewisian gneissic foliation is at a high angle to the frontal hanging wall ramp anticline.

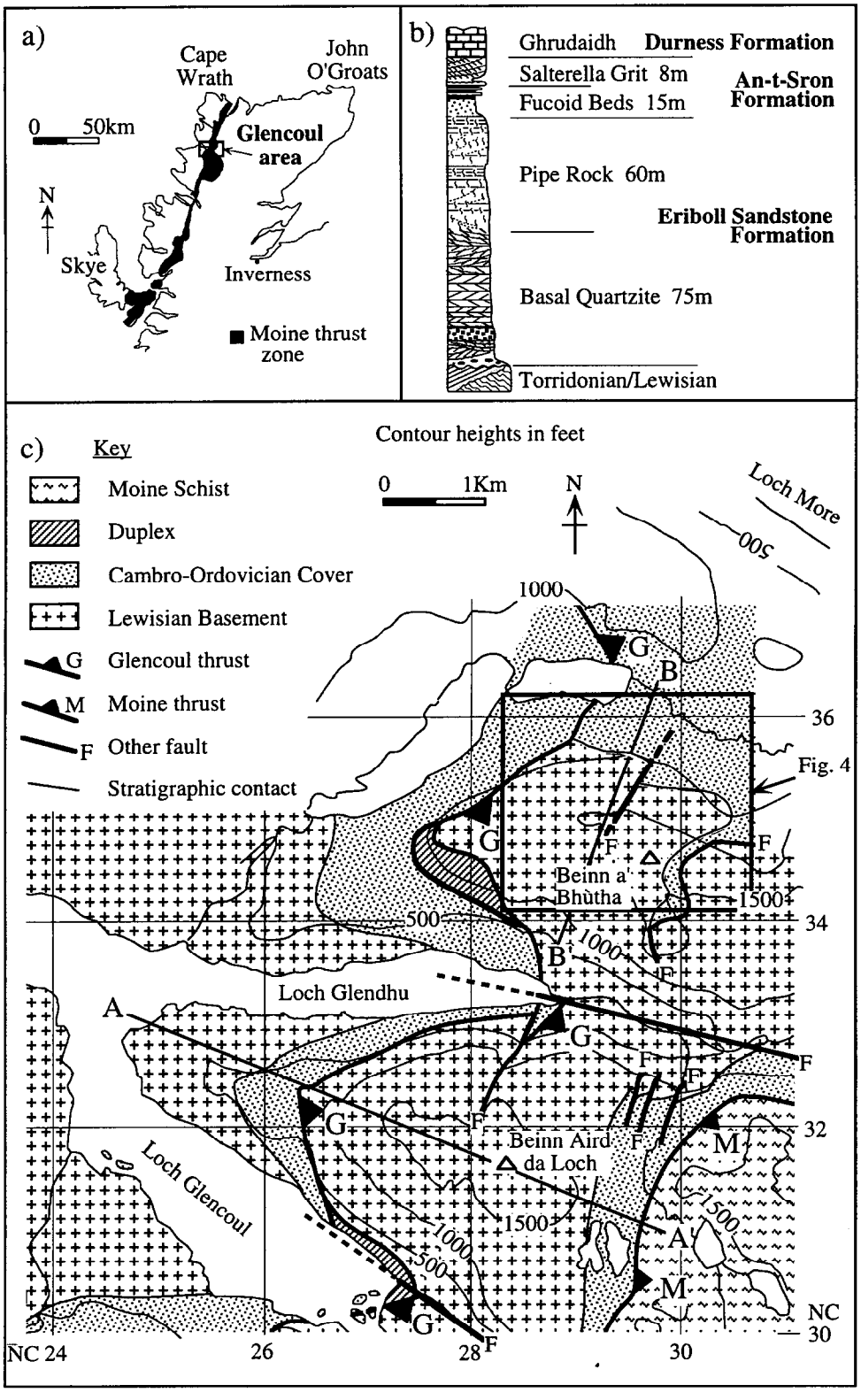

Fig. 3. The Glencoul thrust sheet. (a) Regional location map within the Moine Thrust Zone. (b) Regional stratigraphic column. (c) Geological map of the Glencoul thrust sheet.

Restored thrust sheet geometry

Figure 5(ai) is a strike normal (WNW–ESE) cross-section through the Glencoul thrust sheet, illustrating the location of the basement/cover cut-off by the Glencoul thrust. The positions of sample localities are also shown. The cut-off angle is 20° (see also Elliott and Johnson, 1980, section G–G') and the thickness of basement in the hanging wall flat is approximately 800 m. Assuming that the Glencoul thrust ramp climbs to the top of the Eriboll

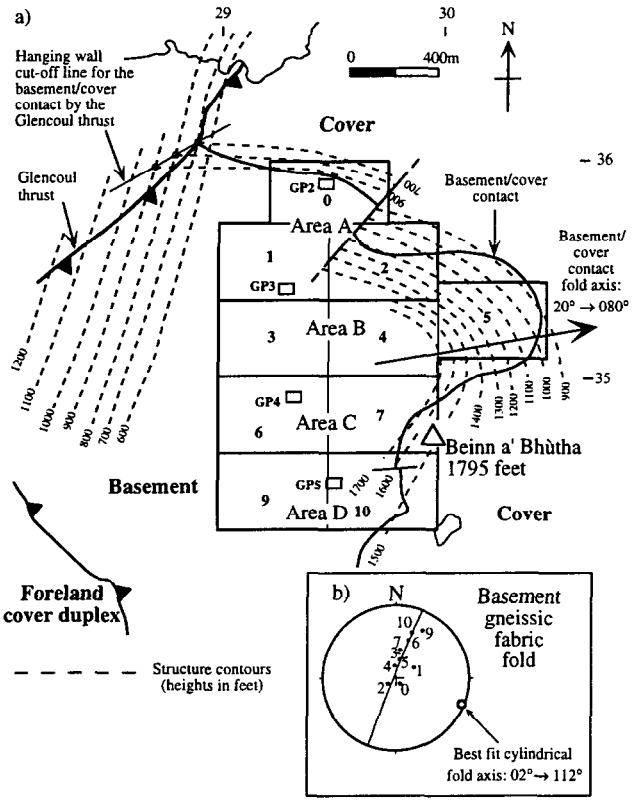

Fig. 4. (a) Map showing the structure of the oblique/lateral monoclinal fold on Beinn a'Bhùtha in relation to the Glencoul thrust, indicating areas of Lewisian basement mapped at 1:2000 scale (see Fig. 3c for location). (b) Stereogram showing the definition of the basement lateral fold, by the orientation distribution of gneissic foliations. Points represent the average pole to between 25 and 150 gneissic foliation measurements for each of the ~300 × 400 m regions.

Sandstone (135 m thick) and becomes a detachment within the Fucoid beds (Elliott and Johnson, 1980), the vertical ramp height is approximately 935 m. From the procedures described in the previous section, parameters for a restored template are: $\theta = 23°$, ramp length (BC) = 2200 m, and $\gamma = 0.41$ (equation 1).

For the lateral cross-section of Fig. 5(bi) the cut-off angle is 45° and the thickness of basement is also approximately 800 m. In this case only restoration by vertical shear is applied, so that the final cut-off angle (θ') is equivalent to the initial ramp dip (θ), and the scale of the fold equals the horizontal span of the original lateral ramp.

The division between the hanging wall ramp regions and the flat region is found using ramp lengths and the position of the cut-off line of the basement/cover contact by the Glencoul thrust. This dividing line between hanging wall flat region and hangingwall ramp regions, shown in Fig. 6, is a curved line, similar to the cut-off line of the basement/cover contact at the Glencoul thrust surface. This line is equivalent to the fold hinge line of a linked hanging wall frontal ramp and lateral ramp anticline. From Fig. 6, the strain history due to emplacement over different thrust bends may be ascertained for any locality in the thrust sheet.

SYN-EMPLACEMENT FABRICS WITHIN THE GLENCOUL THRUST SHEET

This section describes the data obtained from 10 m long line samples through the thrust sheet, and from detailed outcrop scale mapping (30 m × 20 m window samples).

Cataclastic seams

The Lewisian basement of the Glencoul thrust sheet between Loch Glencoul and Beinn a'Bhùtha (Fig. 3c) contains cataclasite seams (Fig. 7) which are absent from the Lewisian in the foreland. These are seams of cemented ultracataclasite fault rock which generally strike normal to the emplacement direction of the thrust sheet (Fig. 8a), although a wide scatter in orientation range about this mean direction occurs. They cross-cut the gneiss as either single seams (e.g. Fig. 7a), 0.5–20 mm thick, or in 100 mm–5 m thick clusters (e.g. Fig. 7b), where individual seams are usually 0.5–5 mm thick. Individual seams vary in length from 100 mm to > 10 m, and show apparent shear displacements of 0–0.5 m, with typical values being 1–10 mm where discernible.

Evidence that the cataclasite seams are syn-thrust emplacement deformation fabrics (Wibberley, 1995) include:

— They occur in the Glencoul thrust sheet, but not in the foreland.

— They cross-cut all Lewisian features.

— They are nowhere observed to cross-cut the Glencoul thrust zone.

— They are rotated by post-emplacement thrust processes, such as breaching of the Glencoul thrust and footwall collapse along the underlying Sole thrust system.

Microstructural evidence (Wibberley, 1995) shows that cataclasite seams in the Lewisian basement originated as quartz/epidote-rich veins (Fig. 7d). These underwent one or more episodes of shearing, which resulted in cataclastic breakdown of the vein material (Fig. 7c, e & f), localised around a central fracture in the vein. Quartz microveins with various orientations cross-cut earlier cataclastic structures within the seams (Fig. 7c). No quartz/epidote veins which have not undergone cataclasis were observed, implying that the generation of these veins is inherently linked to subsequent shearing and cataclasis.

The following model of cataclasite seam evolution in the Lewisian basement accounts for the observed microstructural features:

(1) Fracturing within the Lewisian occurred as a response to either bending or extension (or a combination) within the Glencoul thrust sheet.

(2) Precipitation of epidote and quartz occurred within these fractures to form veins.

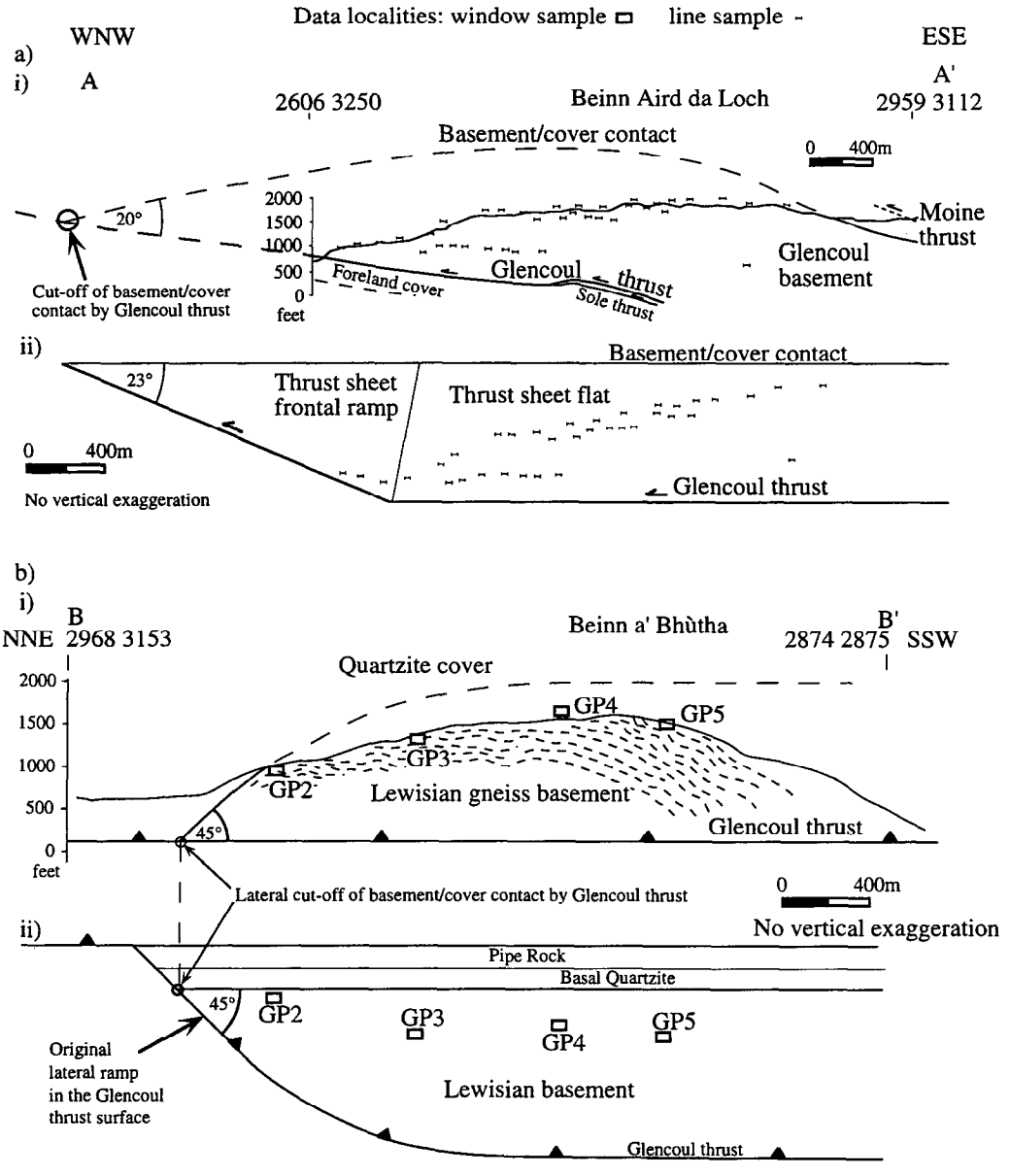

Fig. 5. (a) Frontal cross-sections through the Glencoul thrust sheet (see Fig. 3c for location), showing localities of detailed sampling. (i) Final structure. (ii) Restored structure. (b) Lateral cross-sections through the Glencoul thrust sheet (see Fig. 3c for location). (i) Final structure. (ii) Restored structure.

(3) Shearing of these veins resulted in cataclastic breakdown, often localised in the centre. Later quartz cementation and micro-veining occurred either during continued shearing, or during later events. A later multistage history of shearing events is indicated by the range in cross-cutting quartz microveins.

The Lewisian basement therefore accommodated deformation during the emplacement of the Glencoul thrust sheet by a possibly continuous sequence of fracturing, precipitation and shearing processes which resulted in cataclasite seams formation.

Cataclasite seams rarely show evidence of their slip directions, such as fault surface lineations, hindering kinematic analysis. They do however show offsets of gneissic foliations, and it is often possible to correlate the gneissic banding across a seam. Displacement data is therefore in the form of apparent offsets only. Cataclasite seams from the Glencoul thrust sheet that showed visible offsets were categorised as either 'west side up' (or at least must have had a west side up component) or 'east side up'. The orientations of each of these categories is illustrated in Fig. 8(b) which shows that no systematic relationship between orientation and apparent slip direction is determinable. The presence of cross-cutting seams at any one location allows a comparison of the orientation of earlier cataclasite seams and that of later seams. Figure 8(c) shows the orientations of the earlier (cross-cut) seams and later (cross-cutting) seams for 92 pairs of cross-

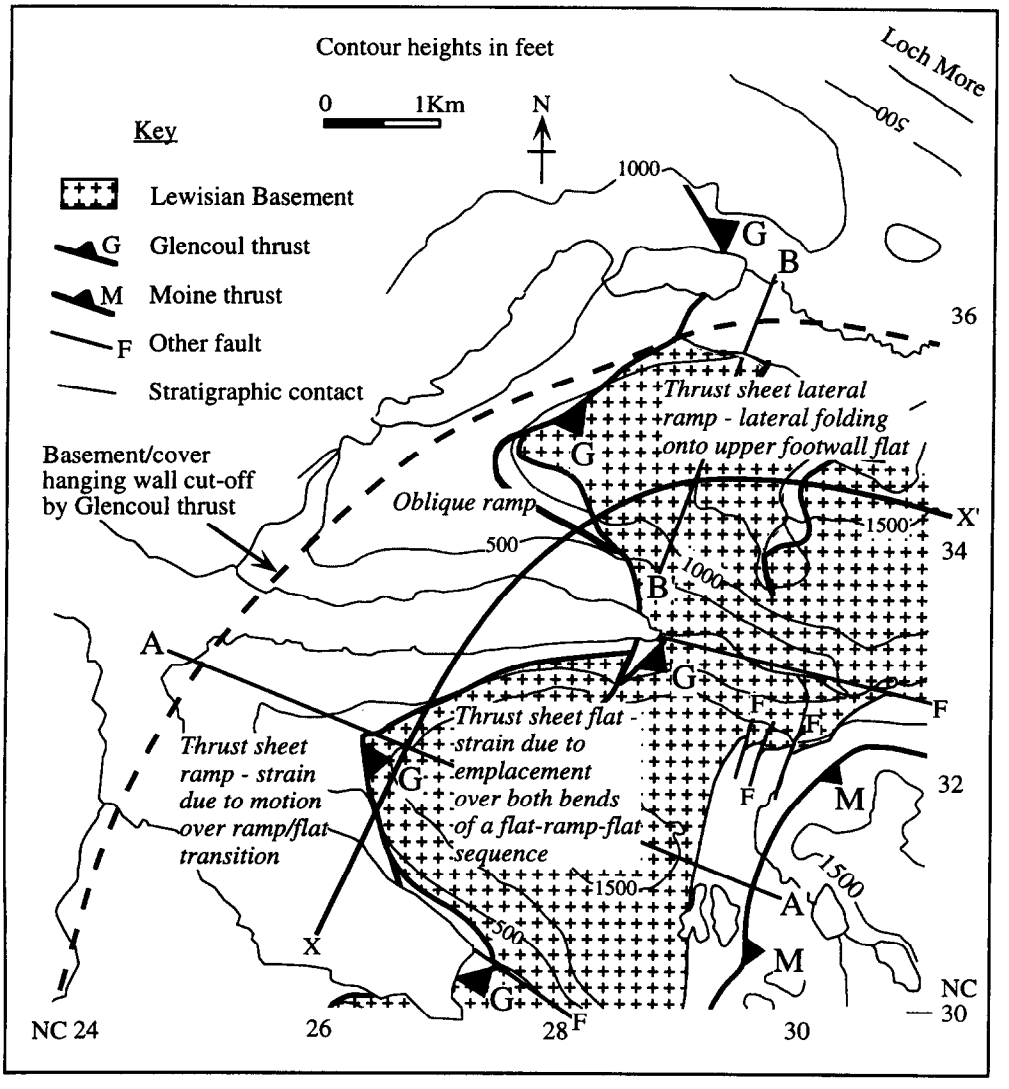

Fig. 6. Map of the Glencoul thrust sheet between Loch Glencoul and Loch More with predicted models of thrust sheet deformation. The map shows the predicted division between thrust sheet ramp the thrust sheet flat (line X–X').

cutting seams throughout the Glencoul thrust sheet. The lack of significant difference in overall orientation suggests there is no systematic relationship for the whole of the Glencoul thrust sheet between the timing of cataclastic seam generation and cataclasite seam orientation.

Data on the frequency distribution of cataclasite seams were collected by line sampling along a frontal (WNW–ESE trending) traverse throughout the Glencoul thrust sheet (line A–A' on Fig. 3c). The frequency variations reflect variations in syn-emplacement bulk strain rather than cataclasite seam thickness, for example, because cataclasite seam frequencies do not show an inversely proportional relationship to seam thickness (Wibberley, 1995). Frequency data (number of cataclasite seams per metre) are averaged from 10 m intervals, for each of the localities in Figs 5(a) and 8(d & e). The results are presented in Fig. 8(d). They show that:

— The highest frequencies are close to the Glencoul thrust in the hanging wall ramp region.

— Similarly high frequencies are not present in hanging wall flat localities relatively close to the Glencoul thrust.

— Frequencies are heterogeneously distributed throughout the Glencoul thrust sheet: some of the higher frequency values occur at relatively large distances from the thrust, whilst small minima occur in the middle of the thrust sheet.

The orientation distribution of cataclasite seams is presented in Fig. 8(d), showing that they are generally steep to sub-vertically dipping, and strike normal to the WNW emplacement direction of the Glencoul thrust. They appear to show a fanning orientation distribution across the traverse, with the exception of the hanging wall ramp region, which possibly reflects rotation by development of the footwall duplex beneath the Glencoul thrust.

The distribution of cataclasite seams was also studied along a lateral (NNE–SSW) traverse across the hanging wall oblique/lateral fold. The orientation and frequency distribution of cataclasite seams is shown in Fig. 9. The

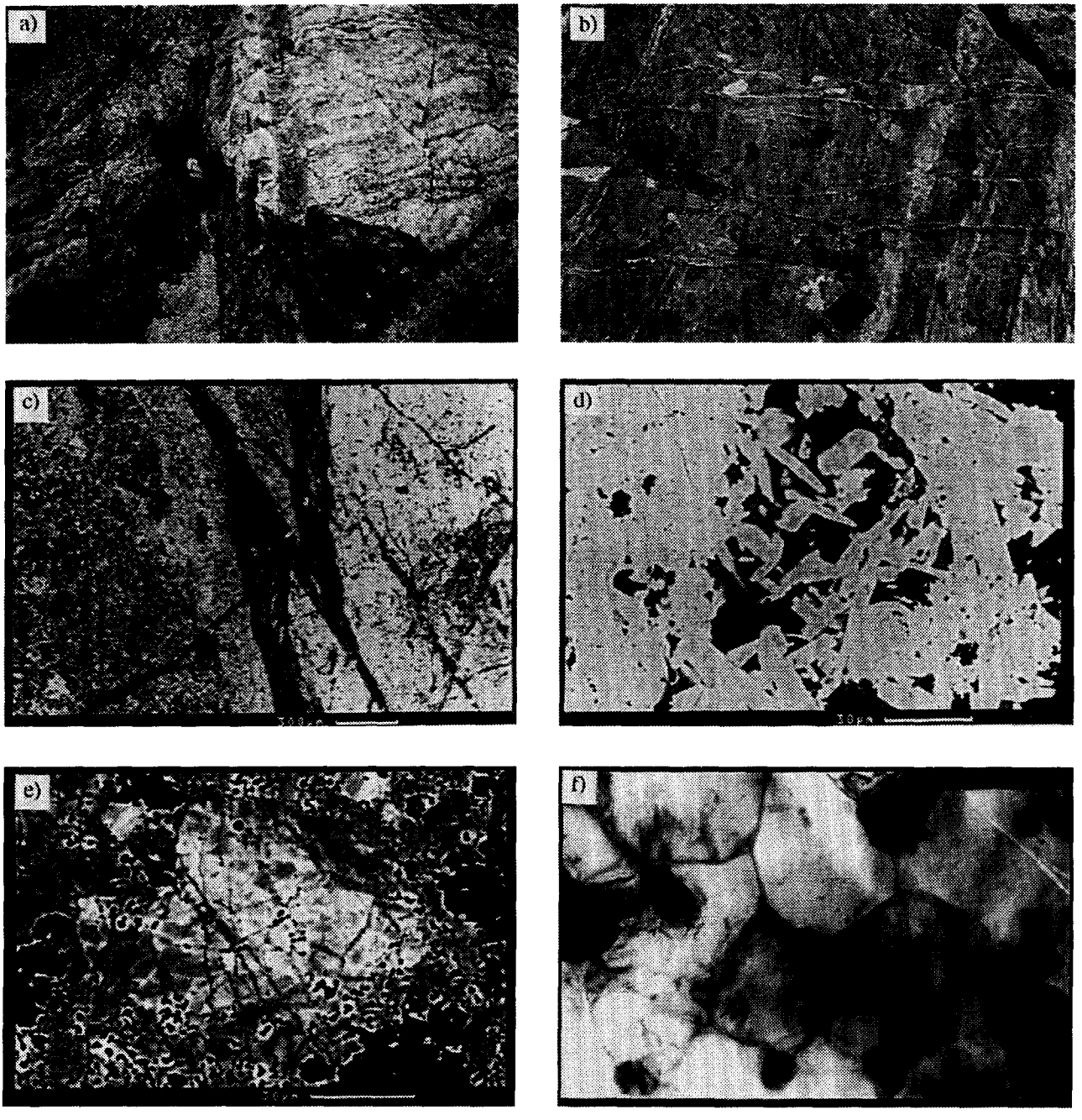

Fig. 7. (a) Photograph of a single cataclasite seam within Lewisian gneissic basement. (b) Photograph of a cluster of cataclasite seams within Lewisian gneissic basement. (c) Backscattered (atomic number contrast) scanning electron (BSE) micrograph of a cataclasite seam, with epidote (light) and quartz (dark), showing intense shearing and multiple microveining. (d) BSE micrograph of needle-like epidote (light) which grew into a pore space, later infilled with quartz (dark). This is interpreted as reflecting early vein-type growth of epidote. (e) BSE micrograph of cataclastic epidote with a wide range of grain sizes. (f) Transmission electron micrograph of cataclastic fault material showing hexagonal quartz grains typical of compacted/cemented cataclasites, where irregular grain boundaries of adjacent quatz fragments have undergone dissolution or grain boundary adjustments to remove porosity (Knipe, 1989, 1990). Width of view: 4 μm.

frequency data show that twice the number of cataclasite seams are present in the hanging wall flat as in the hanging wall lateral ramp. This suggests a significantly different deformation response for the different strain paths (Fig. 1). Orientations show non-systematic variation across the traverse. The orientation data both for area D and for locality GP5 within area D, have a tight clustering. For areas A and B there is a wide scatter, and for area C and GP4 within area C the data appear to exhibit a bimodal orientation pattern. This bimodality for the area C and GP4 data is verified by a statistical test of unimodality versus bimodality of poles to planes on the sphere (Wibberley *et al.*, in prep.). All other data sets were deemed unimodal by the test.

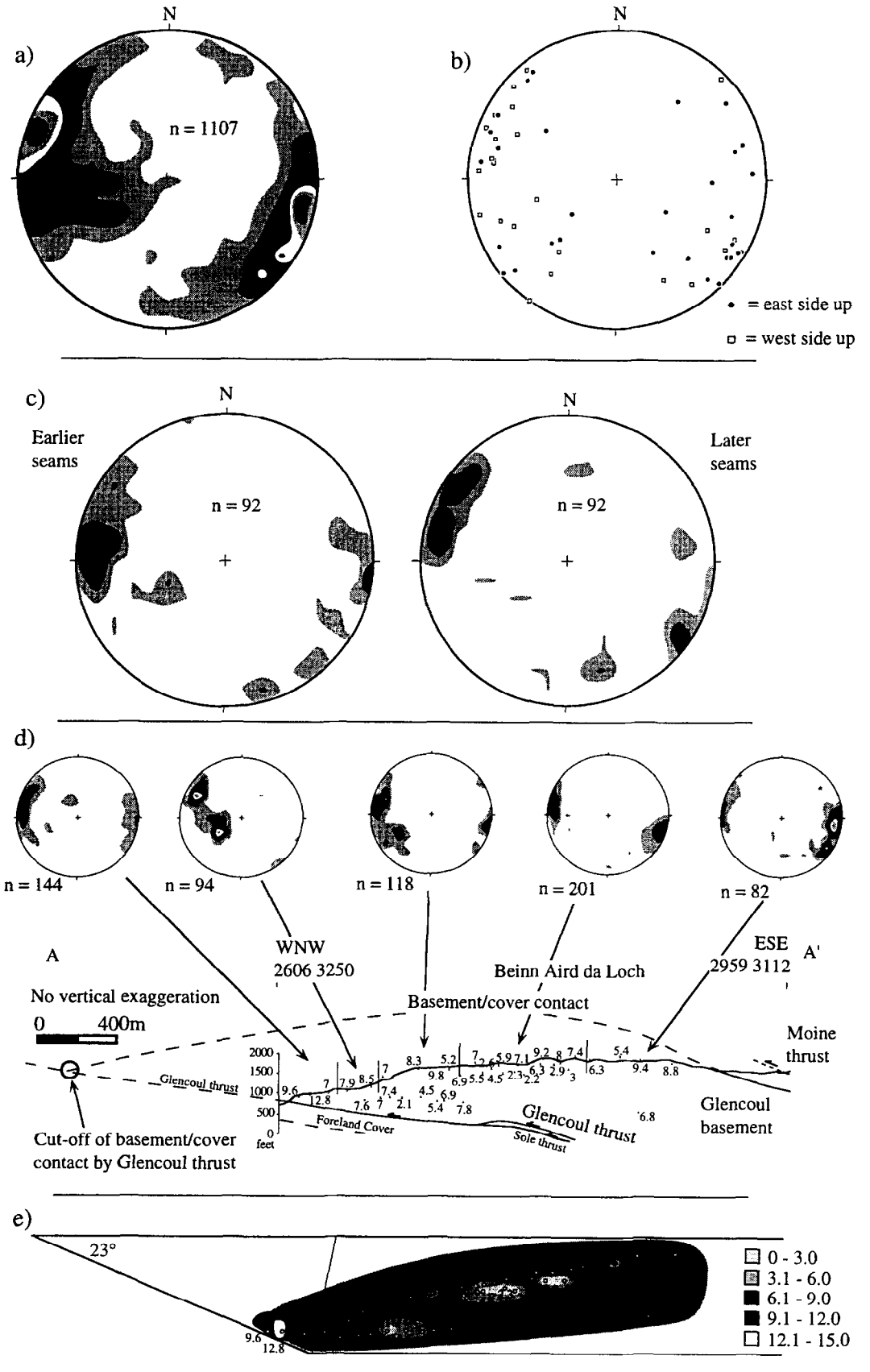

Fig. 8. (a) Equal area lower hemisphere stereogram of poles to cataclasite seams for basement outcrop in the Glencoul thrust sheet between Loch Glencoul and Loch More. (b) Stereogram of poles to cataclasite seams where apparent offsets were recorded. (c) Stereogram of poles to cataclasite seams where cross-cutting relationships were recorded. (d) Cataclasite seam orientation and frequency distribution data on the post-emplacement frontal cross-section. (e) Cataclasite seam frequency data on the restored frontal cross-section.

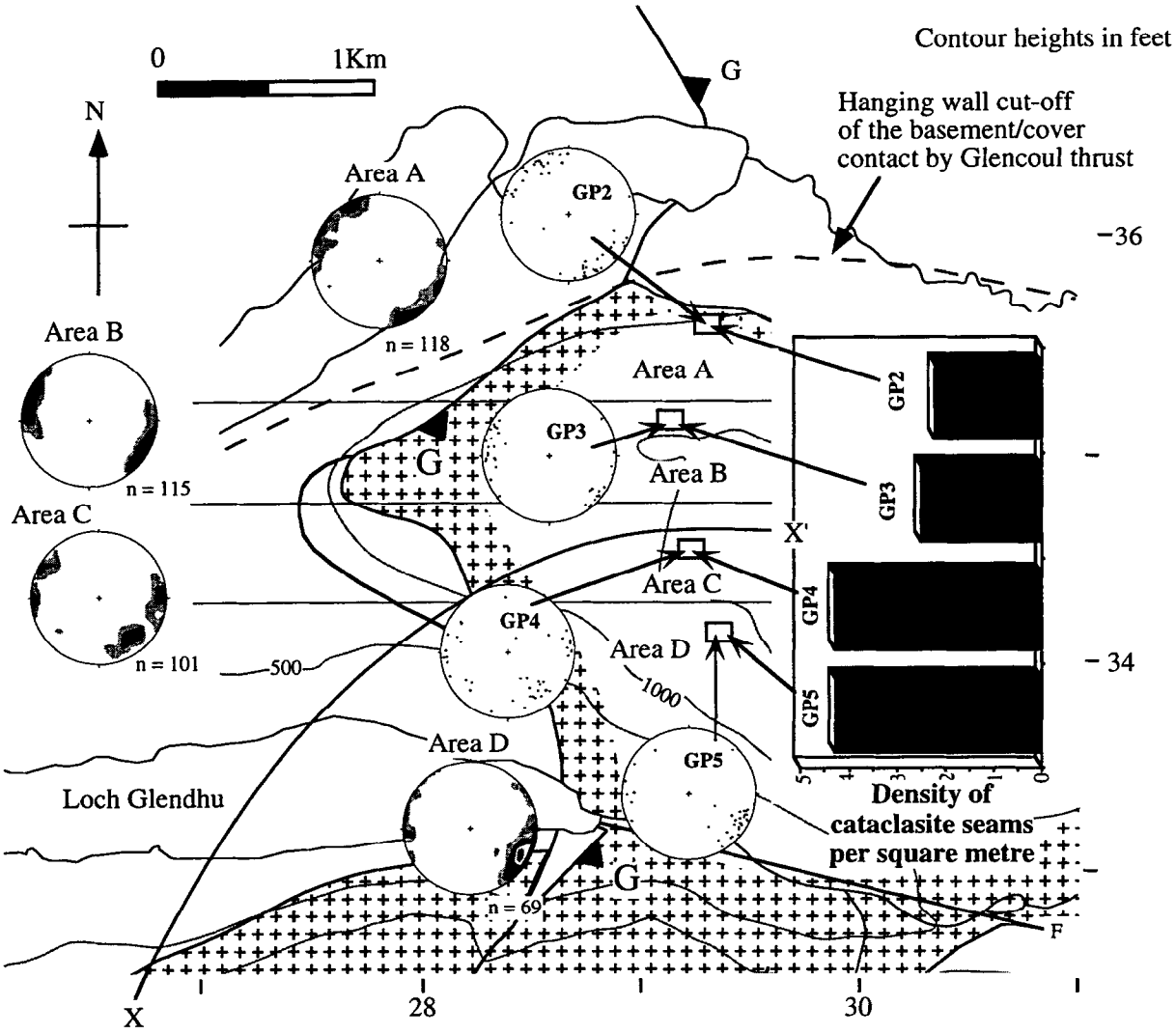

Fig. 9. Spatial and orientation distributions of cataclasite seams along the lateral traverse across the Beinn a'Bhùtha lateral monocline, shown in relation to the predicted strain fields within the Glencoul thrust sheet.

Fractures

Fractures which do not contain an epidote cataclasite fill were also sampled in the lateral traverse across the hanging wall oblique/lateral fold. Figure 10(a) shows the orientation and frequency distributions of these fractures, which are mostly joints. There is no direct evidence for the chronological relationship between them and the cataclasite seams. The data reveal the following points:

— Two sets of fractures are present: a 'frontal' set, striking NNE–SSW, perpendicular to the emplacement direction, and a 'lateral' set, striking WNW–ESE, parallel to the emplacement direction.

— The density of the frontal set of fractures is constant across the fold.

— The density of the lateral fractures decreases across the fold from the lateral cut-off line in towards the middle of the basement culmination.

The relationship between lateral fracture density and position in the lateral fold indicates that fracturing was an important deformation mechanism during folding. The distribution of fractures is summarised in Fig. 10(b). Distance from the thrust is shown not to be a factor affecting lateral fracturing, by examination of lateral fracture frequencies from the frontal traverse (Wibberley, 1995).

INTERPRETATION

The presence of syn-emplacement cataclastic seams suggests that the Lewisian basement in the Glencoul thrust sheet did not behave rigidly during emplacement. Data on the orientation and spatial distributions of these cataclasite seams in the Glencoul thrust sheet were collected from areas within the hanging wall ramp, hanging wall flat, and hanging wall lateral ramp. Figure 1(a) shows how these three regions have different histories of movement over bends in the thrust surface.

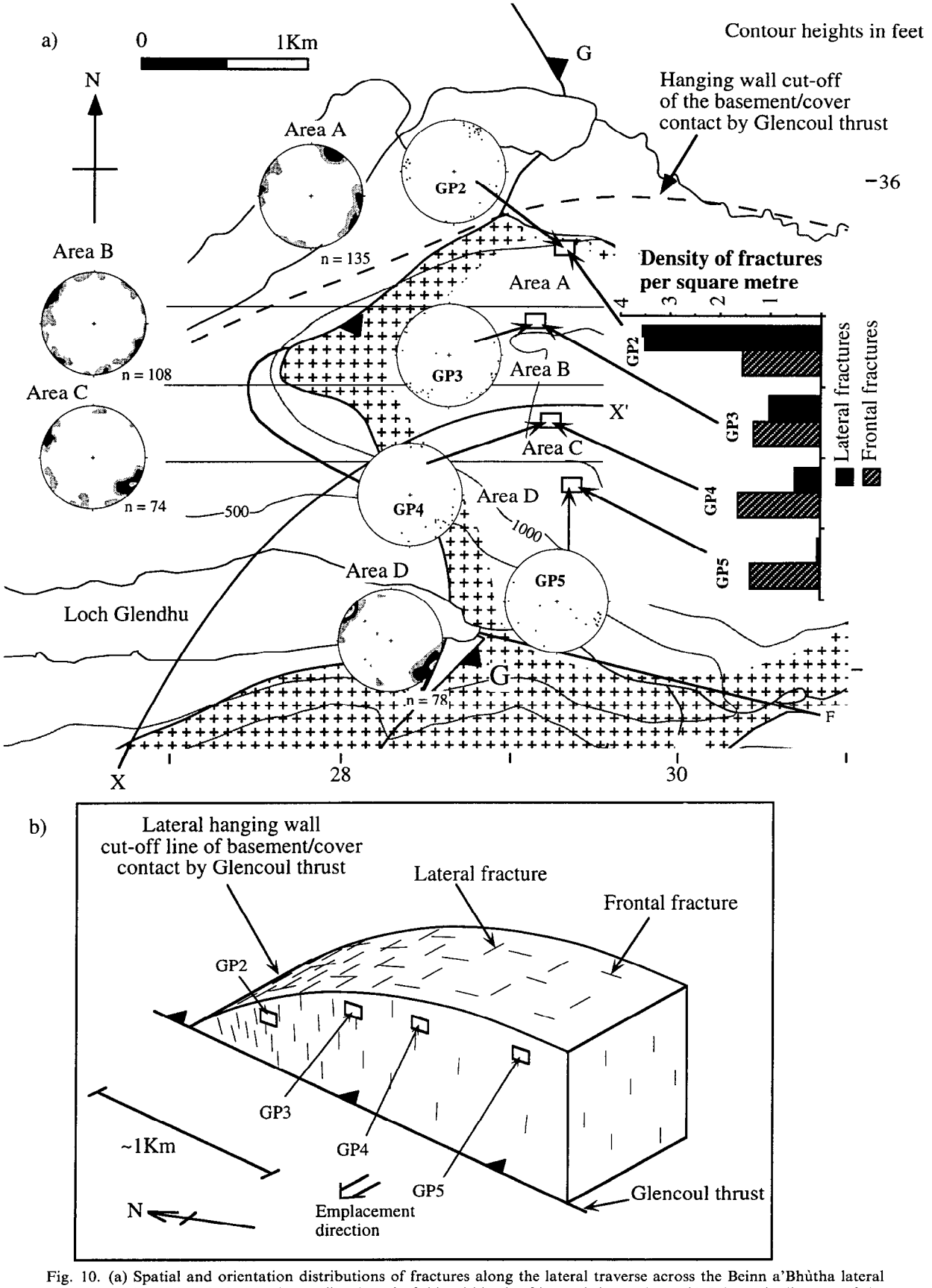

Fig. 10. (a) Spatial and orientation distributions of fractures along the lateral traverse across the Beinn a'Bhùtha lateral monocline, shown in relation to the predicted strain fields within the Glencoul thrust sheet. (b) Schematic diagram of the spatial distributions of fractures in the Lewisian basement with respect to the lateral hanging wall ramp monocline on Beinn a'Bhùtha.

The hanging wall flat region, which moved over two frontal thrust bends, has twice the density of cataclasite seams as the region that moved over the lateral ramp-to-frontal ramp 'corner' bend and one frontal thrust bend. This is evidence that cataclasite seams formed as a response to thrust sheet deformation during movement over frontal bends in the thrust surface (Fig. 11), and implies that movement over a lateral ramp-to-frontal ramp corner bend did not generate cataclasite seams within the thrust sheet. Additionally, this relationship between cataclasite seam density and location on the lateral traverse is inconsistent with cataclasite seam formation by other possible thrust sheet deformation processes. Other possible causative mechanisms introduced earlier may also be ruled out as follows.

(1) Basement response to deformation in the cover by thrust-propagation folding is typically by splay faulting close to the basement cover contact, where the splays form at low angles to the thrust surface (Erslev and Rogers, 1993; Narr, 1993; Schmidt *et al.*, 1993) with essentially little or no rotation occuring within the basement (Narr, 1993). Distributions of cataclastic seams are too widespread throughout the thrust sheet for this.

(2) The final fold geometry of the Glencoul thrust sheet (Fig. 5ai) is a much more open fold than that typical of fault detachment folds described in the literature (Jamison, 1987, 1992). This does not rule out the possibility of small-scale thrust detachment folding localised close to the thrust surface. However, the data are inconsistent with fault detachment folding, because

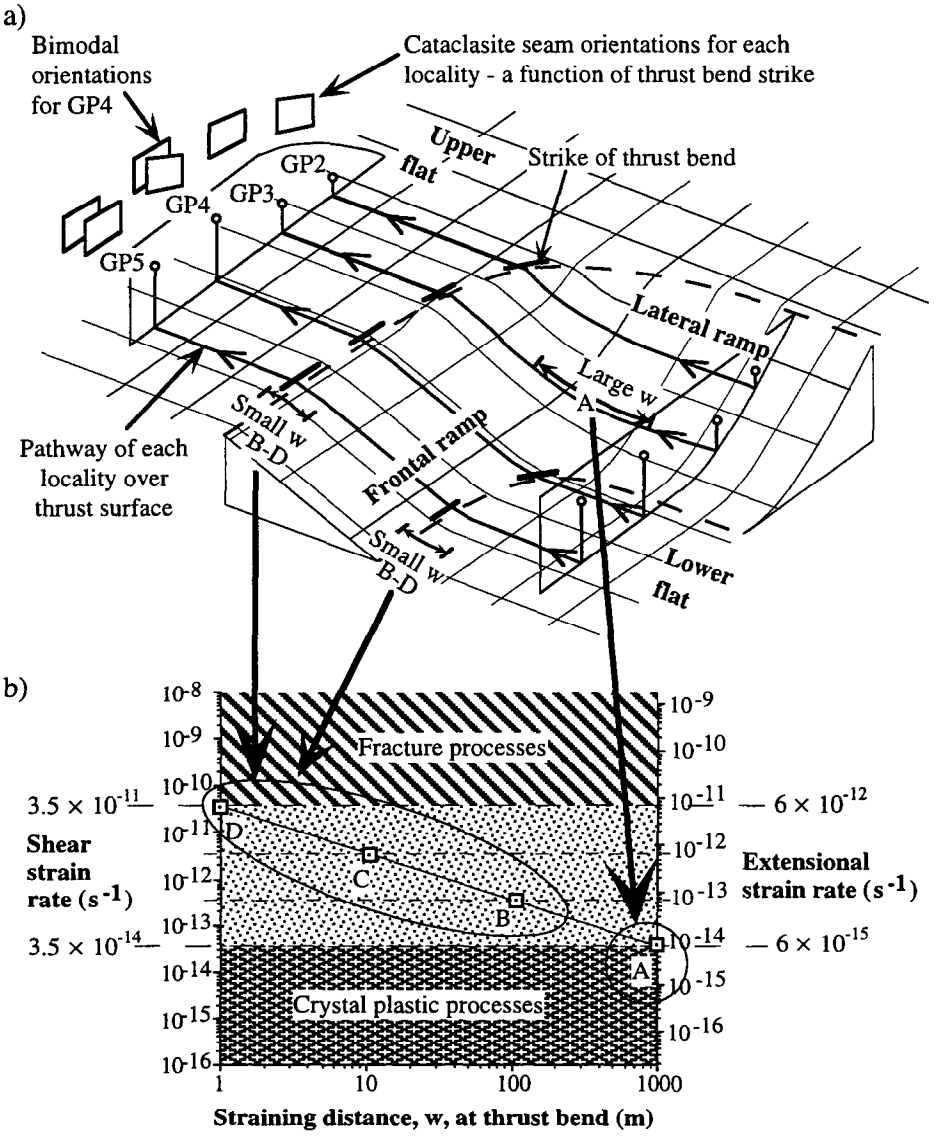

Fig. 11. (a) Schematic diagram of thrust surface geometry showing larger straining distances at the lateral ramp/frontal ramp bend than at the frontal flat/ramp and ramp/flat bends. This schematic diagram illustrates how the orientation range of cataclasite seams is explained by the geometry of the linked frontal/lateral ramp. (b) Theoretical graph of shear and extensional strain rates versus straining distance of the thrust bend, used in determining critical fracture strain rates.

the distribution of cataclasite seams is not at a maximum close to the thrust surface along the hanging wall flat, such as in a zone up to ~100 m above the thrust, which has a zone of rotated dykes close to some parts of the Glencoul thrust (Maobing, 1984).

(3) Initial resistance at the ramp, leading to buckling, may be one cause of the cataclasite seam frequency peak in the hanging wall ramp close to the thrust. However, this mechanism does not explain the persistence of cataclasite seams throughout the thrust sheet flat, nor the orientation and density distributions of the lateral traverse. The frequency peak in the hanging wall ramp is instead considered to be due to additional faulting during movement over a second smaller ramp in the An-t-Sron Formation. Moving over a ramp whose height is much smaller than the thickness of the thrust sheet may induce strains only in a relatively narrow zone adjacent to the thrust surface, rather than throughout the thrust sheet (Wibberley, 1995).

(4) The lack of a universal correlation between cataclasite seam frequency and distance from the thrust suggests they do not reflect a simple strain profile, eliminating thrust parallel shear as a causative mechanism.

(5) Layer-parallel shortening has been invoked as a cause of ductile structures within basement thrust sheets in the Blue Ridge anticlinorium (Mitra, 1979) and in the Aar massif (Choukroune and Gapais, 1983; Wibberley, 1995), with the heterogeneous development of anastomosing deformation zones reflecting bulk flattening (Bell, 1981; Choukroune and Gapais, 1983). Similar geometric and kinematic fault arrangements to these anastomosing patterns have been described by Reches (1983) and Reches and Dieterich (1983), and are consistent with the broad scatter in cataclasite seam orientations about a steep bisector perpendicular to the emplacement direction. Layer-parallel shortening would not, however, give rise to the spatial density distributions described above in the lateral traverse. Orientation scatter may instead be ascribed to the complicated small-scale pre-existing heterogeneities within the Lewisian.

Frontal folding of the hanging wall lateral ramp region has contributed to the generation of structures within the lateral monocline. The cataclasite seams, formed at the upper ramp-to-flat bend, must have formed after lateral folding and have therefore formed in their current orientations (corrected for foreland tilt). This is corroborated by the orientations of cataclasite seams, which vary across the fold more than predicted by the simple rotation of pre-existing planes during lateral folding. A comparison of the cataclasite seam orientations with the pattern of thrust bends (Fig. 11a) suggests that this swing in orientations is a result of thrust sheet emplacement over a curved ramp-to-flat bend, so that cataclasite seams form strike-parallel to the trend of the bend. This explains the bimodality of cataclasite seam orientation data for region C and GP4, at the edge of the fold, whilst all the other localities have unimodal orientation distributions. Emplacement over an oblique ramp may result in movement over two bends of different strikes. If cataclasite seams form strike-parallel to the trend of the thrust bend, this will result in two orientation groups of cataclasite seams (Fig. 11a).

Given that the curvature on the lateral ramp-to-frontal ramp corner bend is much broader (larger straining distance, w) than on the frontal thrust bends (Wibberley, 1995) (Fig. 11a), the dependence of cataclasite seam densities on thrust bend sequence suggests that the straining distance at thrust bends dictates the generation of cataclasite seams. Knipe (1985) shows how the straining distance of a thrust bend controls the strain rate associated with movement over that thrust bend. If the strain rate controls cataclasite seam formation, estimates of the straining distance at the frontal and lateral 'corner' bends in the thrust surface can be used to place constraints on the strain rates necessary for cataclasite seam generation. As cataclasite seam formation is a fracture process, these strain rates are interpreted as maximum and minimum estimates of the critical strain rate required for fracture failure in the Lewisian basement. A straining distance (w) of $1000\ \text{m} \pm 500\ \text{m}$ is estimated for the lateral ramp-to-frontal ramp bend, based on lateral ramp curvature (Fig. 5bii), and the curvature of the basement/cover cut-off (Fig. 6). Estimates of frontal thrust bend curvature are more difficult to obtain, but for a ramp angle of 23° and a vertical ramp height of 800 m, straining distances are considered unlikely to be less than 1–2 m or greater than 100–200 m for each bend. If the displacement rate on the Glencoul thrust is in the order of $1 \times 10^{-10}\ \text{m s}^{-1}$ ($3\ \text{mm yr}^{-1}$) (Knipe, 1990), the outside limits in the estimates of critical strain rates for fracture failure would have been $3.5 \times 10^{-11}\ \text{s}^{-1}$ ($w = 1$ m at which fracture failure occurred) to $3.5 \times 10^{-14}\ \text{s}^{-1}$ ($w = 1000$ m at which fracture failure did not occur) (Fig. 11b). Shear-related extensional strain rates may similarly be calculated, using the geometric relationship between shear strain and maximum line length extension within a homogeneous shear zone (Ramsay and Huber, 1983). Extensional strain rates derived are $6 \times 10^{-12}\ \text{s}^{-1}$ to $6 \times 10^{-15}\ \text{s}^{-1}$. These estimates apply to Lewisian basement at lower greenschist facies conditions of 250–300°C and 5–9 km depth (Knipe, 1990).

The set of fractures striking parallel to the fold axis and fanning across the fold is evidence that the Lewisian basement responded to lateral folding or vertical shear, at least in part, by fracturing.

CONCLUSIONS

Models have been analysed for thrust sheet deformation by steep shear above thrust bends. The prediction of strains associated with thrust-bend folding indicate that

the shear strain is at a minimum when the shear plane bisects the ramp/flat angle. This is considered most important in isotropic rocks or for thrust sheets with highly irregular anisotropic structure (e.g. Lewisian basement).

Strain associated with deformation during thrust sheet movement over each frontal bend was accommodated in the Lewisian basement of the Glencoul thrust sheet by the generation of epidote- and quartz-filled cataclasite seams. These cataclasite seams formed with a strike which is perpendicular to the trend of the thrust bend. A model for their generation in relation to frontal ramp deformation is presented in Fig. 12. The orientations and kinematics of these predicted faults in this model are similar to those intuitively suggested by Elliott (1976b). Emplacement of the Glencoul thrust sheet over a lateral ramp/frontal ramp 'corner' bend did not generate sufficiently high strain rates within the thrust sheet for this mechanism of deformation. Estimation of the straining distances of the thrust bends which did, or did not, generate sufficiently high strain rates for cataclasite seam formation, leads to a determination of the minimum (critical) strain rates required for fracture failure in the Lewisian basement. These are in the order of 10^{-11} to 10^{-14} s^{-1} for shear strain rates and 10^{-12} to 10^{-15} s^{-1} for extensional strain rates at the conditions under which the Glencoul thrust sheet was emplaced (250–300°C, 5–9 km burial depth). Lateral folding of the hanging wall lateral ramp during emplacement on the higher footwall flat was accommodated in the Lewisian basement at least in part by fracturing.

This paper presents a method for estimating critical strain rates required for fracture failure. The method does not rely on extrapolation from experimental to geological time scales, and demonstrates the power of integrating field data with theoretical modelling. Due to this approach, the conclusions drawn here on strain rates and deformation mechanisms are of broader interest to structural geologists in general than only to those interested in fault-related folding.

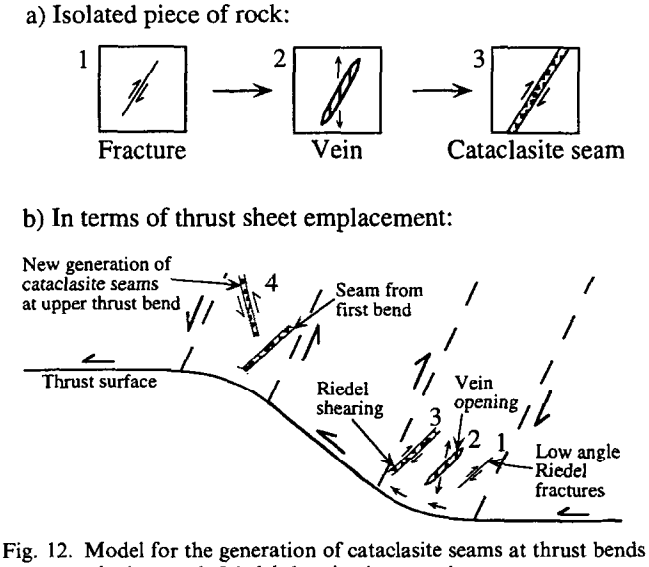

Fig. 12. Model for the generation of cataclasite seams at thrust bends by low angle Riedel shearing in steep shear zones.

Acknowledgements—This work formed part of a NERC funded Ph.D. supervised by Rob Knipe and Rob Butler who are thanked for their input. I am also grateful to the other people in the Earth Sciences department at Leeds who have given me feedback. The manuscript was greatly improved after reviews from Donald Fisher, Gautam Mitra and Nicholas Woodward. John Gibson, Willie on the Statesman, and the Wester Ross fish farmers from Kylesku are thanked for giving me numerous lifts across Loch Glencoul. Finally I would like to dedicate this paper to Will Ramsbottom, who's encouragement and enthusiasm for fieldwork was of great benefit to me.

REFERENCES

Apotria, T. G. (1989) Vector analysis of fault bends and intersecting faults: Discussion. *Journal of Structural Geology* **11**, 503–505.

Apotria, T. G. (1995) Thrust sheet rotation and out-of-plane strains associated with oblique ramps: An example from the Wyoming salient, U.S.A. *Journal of Structural Geology* **17**, 647–662.

Apotria, T. G., Snedden, W. T., Spang, J. H. and Wiltschko, D. V. (1992) Kinematic models of deformation at an oblique ramp. In *Thrust Tectonics*, ed. K. R. McClay, pp. 141–154. Chapman and Hall, London.

Bell, T. H. (1981) Foliation development—the contribution, geometry and significance of progressive, bulk, inhomogeneous shortening. *Tectonophysics* **75**, 273–296.

Berger, P. and Johnson, A. M. (1980) First-order analysis of deformation of a thrust sheet moving over a ramp. *Tectonophysics* **70**, T9–T24.

Bertini, G., Marcucci, M., Nevini, R., Passerini, P. and Sguazzoni, G. (1985) Patterns of faulting in the Mt Blanc granite. *Tectonophysics* **111**, 65–106.

Boyer, S. E. and Elliott, D. (1982) Thrust systems. *Bulletin of the American Association of Petroleum Geologists* **66**, 1196–1230.

Butler, R. W. H. (1982a) The terminology of thrust structures. *Journal of Structural Geology* **4**, 239–245.

Butler, R. W. H. (1982b) Hanging wall strain: A function of duplex shape and footwall topography. *Tectonophysics* **88**, 235–246.

Butler, R. W. H. (1984) Structural evolution of the Moine thrust belt between Loch More and Glendhu Sutherland. *Scottish Journal of Geology* **20**, 161–179.

Choukroune, P. and Gapais, D. (1983) Strain pattern in the Aar granite (Central Alps): orthogneiss developed by bulk homogeneous flattening. *Journal of Structural Geology* **5**, 411–418.

Coward, M. P. and Kim, J. H. (1981) Strain within thrust sheets. In *Thrust and Nappe Tectonics*, eds K. R. McClay and N. J. Price, Vol. 9, pp. 275–292. Special Publications of the Geological Society, London.

Coward, M. P., Kim, J. H. and Parke, J. (1980) A correlation of Lewisian structures and their displacement across the lower thrusts of the Moine thrust zone N.W. Scotland. *Proceedings of the Geological Association, London* **91**, 327–337.

Cox, A. and Hart, R. B. (1986) *Plate Tectonics: How it works*. Blackwell Scientific, Oxford.

Dahlstrom, C. D. A. (1969) Balanced cross-sections. *Canadian Journal of Earth Sciences* **6**, 743–757.

Dahlstrom, C. D. A. (1970) Structural geology in the eastern margin of the Canadian Rocky mountains. *Bulletin of Canadian Petroleum Geology* **18**, 332–406.

Dominic, J. B. and McConnell, D. A. (1994) The influence of structural lithic units in fault-related folds Seminoe Mountains, Wyoming, U.S.A. *Journal of Structural Geology* **16**, 769–779.

Elliott, D. (1976a) The motion of thrust sheets. *Journal of geophysical Research* **81**, 949–963.

Elliott, D. (1976b) The energy balance and deformation mechanisms of thrust sheets. *Philosophical Transactions of the Royal Society, London* **A283**, 289–312.

Elliott, D. and Johnson, M. R. W. (1980) Structural evolution in the northern part of the Moine thrust belt, N.W. Scotland. *Transactions of the Royal Society of Edinburgh: Earth Sciences* **71**, 69–96.

Ernst, W. G. (1973) Interpretative synthesis of metamorphism in the Alps. *Geological Society of America Bulletin* **84**, 2053–2078.

Erslev, E. A. and Rogers, J. L. (1993) Basement-cover geometry of Laramide fault-propagation folds. In *Laramide Basement Deformation in the Rocky Mountain Foreland of the Western United States*, eds C. J. Schmidt, R. B. Chase and E. A. Erslev, Geological Society America Special Paper. 280, pp. 125–145.

Evans, J. P. (1988) Deformation mechanisms in granitic rocks at shallow crustal levels. *Journal of Structural Geology* **10**, 437–443.

Evans, J. P. (1990) Textures, deformation mechanisms, and the role of fluids in the cataclastic deformation of granitic rocks. In *Deformation Mechanisms, Rheology and Tectonics*, eds R. J. Knipe and E. H. Rutter, Vol. 54, pp. 29–30. Special Publications of the Geological Society, London.

Evans, J. P. (1993) Deformation mechanisms and kinematics of a crystalline-cored thrust sheet: The EA thrust system, Wyoming. In *Laramide Basement Deformation in the Rocky Mountain Foreland of the Western United States*, eds C. J. Schmidt, R. B. Chase and E. A. Erslev, Geological Society America Special Paper 280, pp. 147–161.

Fischer, M. W. and Coward, M. P. (1982) Strains and folds within thrust sheets: an analysis of the Heilam sheet, Northwest Scotland. *Tectonophysics* **88**, 291–312.

Frey, M., Hunzeker, J. C., Frank, W., Bocquet, J., Dal Piaz, G. V., Jäger, E. and Niggli, E. (1974) Alpine Metamorphism of the Alps. *Schweizerische Mineralogische and petrographische Mittenhungar* **51**, 247–289.

Frey, M., Schmid, S. M. and Stahel, A. (1993) Symposium metamorphism and deformation: Introduction. *Schweizerische Mineralogische and petrographische Mittenhungar* **73**, 175–176.

Harris, L. D. (1970) Details of thin-skinned tectonics, in parts of Valley and Ridge and Cumberland Plateau provinces of the southern Appalachians. In *Studies of Appalachian Geology: Central and Southern*, eds G. W. Fisher, F. J. Pettijohn, J. C. Read and K. N. Weaver, pp. 161–173.

Hatcher, R. D. J. and Hooper, R. J. (1992) Evolution of crystalline thrust sheets in the internal parts of mountain chains. In *Thrust Tectonics*, ed. K. R. McClay, pp. 217–232. Chapman and Hall, London.

Hedlund, C. A., Anastasio, D. J. and Fisher, D. M. (1994) Kinematics of fault-related folding in a duplex, Lost River Range Idaho, U.S.A. *Journal of Structural Geology* **16**, 571–584.

Jamison, W. J. (1987) Geometric analysis of fold development in overthrust terranes. *Journal of Structural Geology* **9**, 207–219.

Jamison, W. R. (1992) Stress controls on fold thrust style. In *Thrust Tectonics*, ed. K. R. McClay, pp. 155–164. Chapman and Hall, London.

Knipe, R. J. (1985) Footwall geometry and the rheology of thrust sheets. *Journal of Structural Geology* **7**, 1–10.

Knipe, R. J. (1989) Deformation mechanisms—Recognition from natural tectonites. *Journal of Structural Geology* **11**, 127–146.

Knipe, R. J. (1990) Microstructural analysis and tectonic evolution in thrust systems: examples from the Assynt region of the Moine Thrust Zone, Scotland. In *Deformation Mechanisms in Ceramics, Minerals and Rocks*, eds D. J. Barber and P. G. Meredith, pp. 228–261.

Maobing, L. (1984) Geometry of deformation adjacent to the Glencoul thrust at Loch Glencoul Sutherland. *Scottish Journal of Geology* **20**, 1–8.

McCaig, A. M. (1988) Vector analysis of fault bends and intersecting faults. *Journal of Structural Geology* **10**, 121–124.

McClay, K. R. (1992) Glossary of thrust tectonics terms. In: *Thrust Tectonics*, ed. K. R. McClay, pp. 419–433. Chapman and Hall, London.

McClay, K. R. and Coward, M. P. (1981) The Moine Thrust Zone: an overview. In *Thrust and Nappe Tectonics*, eds K. R. McClay and N. J. Price, Vol. 9, pp. 241–260. Special Publications of the Geological Society, London.

McNaught, M. A. and Mitra, G. (1996) The use of finite strain data in constructing a retrodeformable cross-section of the Meade thrust sheet, southeastern Idaho, U.S.A. *Journal of Structural Geology* **18**, 573–583.

Meyre, C. and Puschnig, A. R. (1993) High-pressure metamorphism and deformation at Trescolmen, Adula nappe Central Alps. *Schweiz. Mineral. Petrogr. Mitt.* **73**, 277–283.

Mitra, G. (1979) Ductile deformation zones in Blue Ridge basement rocks and estimation of finite strains. *Geological Society of America Bulletin* **90**, 935–951.

Mitra, G. (1984) Brittle to ductile transition due to large strains along the White Rock thrust Wind River Mountains, Wyoming. *Journal of Structural Geologists* **6**, 51–61.

Mitra, S. (1990) Fault-propagation folds: Geometry, kinematic evolution, and hydrocarbon traps. *Bulletin of the American Association of Petroleum Geologists* **74**, 921–945.

Mitra, G. (1992a) Deformation of Granitic Basement Rocks along Fault Zones at Shallow to Intermediate Crustal Levels. In *Structural Geology of Fold and Thrust Belts*, eds S. Mitra and G. W. Fisher, pp. 123–144. Johns Hopkins Press, Baltimore.

Mitra, S. (1992b) Balanced Structural Interpretations in Fold and Thrust Belts. In *Structural Geology of Fold and Thrust Belts*, eds S. Mitra and G. W. Fisher, pp. 53–77. Johns Hopkins Press, Baltimore.

Mitra, G. (1994) Strain variation in thrust sheets across the Sevier fold-and-thrust belt (Idaho–Utah–Wyoming): implications for section restoration and wedge taper evolution. *Journal of Structural Geology* **16**, 585–602.

Mosar, J. and Suppe, J. (1992) Role of shear in fault-propagation folding. In *Thrust Tectonics*, ed. K. R. McClay, pp. 123–132. Chapman and Hall, London.

Narr, W. (1993) Deformation of basement inbasement-involved, compressive structures. In *Laramide Basement Deformation in the Rocky Mountain Foreland of the Western United States*, eds C. J. Schmidt, R. B. Chase and E. A. Erslev, Geological Society of America Special Paper 280, pp. 107–123.

Peach, B. N., Horne, J., Gunn, W., Clough, C. T. and Hinxman, L. W. (1907) *The Geological Structure of the North-West Highlands of Scotland.* Memoirs of the Geological Survey, Great Britain.

Ramsay, R. G. and Huber, M. I. F. (1983) *The Techniques of Modern Structural Geology*. Academic Press.

Reches, Z. (1983) Faulting of rocks in three-dimensional strain fields II. Theoretical analysis. *Tectonophysics* **95**, 133–156.

Reches, Z. and Dieterich, J. H. (1983) Faulting of rocks in three-dimensional strain fields. I. Failure of rocks in polyaxial, servo-control experiments. *Tectonophysics* **95**, 111–132.

Rich, J. L. (1934) Mechanics of low-angle overthrust faulting illustrated by Cumberland thrust block, Virginia, Kentucky and Tennessee. *Bulletin of the American Association of Petroleum Geologists* **18**, 1584–1596.

Sanderson, D. J. (1982) Models of strain variation in nappes and thrust sheets: a review. *Tectonophysics* **88**, 201–233.

Schmidt, C. J., Evans, J. P., Harlan, S., Batatian, D., Derr, D., Dubois, M., Malizzi, L., McDowell, R., Nelson, G, Parke, M. and Weberg, E. (1993) Mechanical behaviour of basement rocks, Scarface thrust, central Madison Range, Montana. In *Basement Deformation in Rocky Mountain Foreland Structures*, eds C. J. Schmidt, R. Chase and E. Erslev, Geological Society of America Special Paper 280. pp. 89–105.

Serra, S. (1977) Styles of deformation on the ramp regions of overthrust faults. In *Wyoming geological Association, 29th Annual Field Conference Guidebook*, pp. 487–498.

Spang, J. H. and Evans, J. P. (1988) Geometrical and mechanical constraints on basement-involved thrusts in the Rocky Mountain foreland province. In *Interaction of the Rocky Mountain foreland and the Cordilleran thrust belt*, eds C. J. Schmidt and W. J. Perry, Memoirs Geological Society America. 171, pp. 41–51.

Suppe, J. (1983) Geometry and Kinematics of Fault-bend Folding. *American Journal of Science* **283**, 684–721.

Suppe, J. and Medwedeff, D. A. (1984) Fault-propagation folding. *Geological Society of America Abstracts with Programs* **16**, 670.

Wibberley, C. A. J. (1995) Basement Involvement and Deformation in Foreland Thrust Belts. Unpublished Ph.D. dissertation, University of Leeds.

Wiltschko, D. V. (1979) A mechanical model for thrust sheet deformation at a ramp. *Journal of geophysical Research* **84**, 1091–1104.

Wojtal, S. G. (1992) One-dimensional models for plane and non-plane power-law flow in shortening and elongated thrust zones. In *Thrust Tectonics*, ed. K. R. McClay, pp. 41–52. Chapman and Hall, London.